LBNL-39758
UC-406

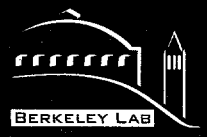

ERNEST ORLANDO LAWRENCE
BERKELEY NATIONAL LABORATORY

Coplanar-Grid Detector with Single-Electrode Readout

M. Amman and P.N. Luke
Engineering Division

April 1997
To be presented at the
Optical Science, Engineering and Instrumentation '97,
San Diego, CA,
July 27–August 1, 1997,
and to be published in
the Proceedings

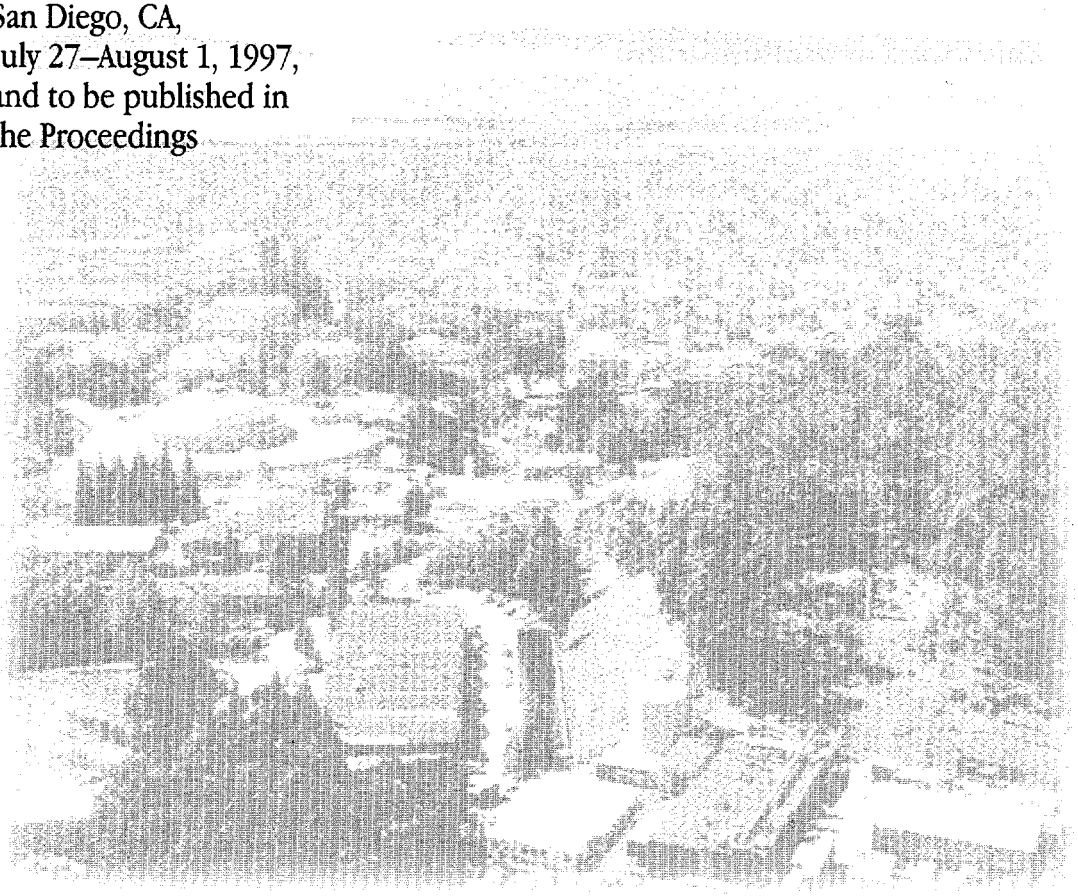

LBNL-39758
UC-406

Coplanar-Grid Detector with Single-Electrode Readout

M. Amman and P.N. Luke

Engineering Division
Ernest Orlando Lawrence Berkeley National Laboratory
University of California
Berkeley, California 94720

April 1997

This work was supported by the Director, Office of Energy Research, Biological and Environmental Research, of the U.S. Department of Energy under Contract No. DE-AC03-76SF00098.

Coplanar-grid detector with single-electrode readout

M. Amman and P. N. Luke

Ernest Orlando Lawrence Berkeley National Laboratory
University of California
Berkeley, California 94720

ABSTRACT

The coplanar-grid technique provides substantial spectral performance improvement over that of conventional detector designs and electronics when applied to gamma-ray detectors based on compound semiconductors. The technique realizes this improvement by measuring the difference between the induced charge signals from two interdigitated coplanar-grid electrodes. By adjusting the relative gain between the two grid signals prior to subtraction, the difference signal can be made less sensitive to the poor carrier transport properties of the detector material and thus improve the spectral response of the detector. In this paper, we discuss a variation of the coplanar-grid method in which the signal from only one grid electrode is read out. The signal response is optimized by changing the relative areas of the two grid electrodes and the bias applied across the detector. In this scheme, only one preamplifier is needed and signal subtraction is not necessary. This eliminates the electronic noise contribution from the additional preamplifier used in the normal coplanar-grid implementation, and conventional single-amplifier detector electronics can be used. Experimental results using CdZnTe detectors are presented.

Keywords: gamma-ray detector, coplanar grid, single-electrode readout, compound semiconductor, CdZnTe

1. INTRODUCTION

Wide-bandgap compound semiconductors have shown great promise for use in room-temperature gamma-ray detectors.[1-4] However, detectors based on these materials typically have poor spectral response when conventional detector configurations and electronics are used. This primarily results from the hole transport characteristics of the semiconductor materials being substantially inferior to those of the electron. Consequently, the holes are collected much less efficiently, which causes the amplitude of the detector signal to vary as a function of the depth of gamma-ray interaction. It has been shown though that by properly designing the charge sensing electrode on a detector, the signal response can be modified such that the signal amplitude variation is greatly reduced.[5-10] The coplanar-grid technique developed in recent years makes use of this principle to achieve significant improvements in the spectral response of CdZnTe detectors.[6,11] It uses two interdigitated electrodes on the detector for charge sensing. The desired signal response is obtained by subtracting the induced signals on the two grid electrodes. By changing the relative gain of the two signals before subtraction, the detector response can be effectively tuned to match the charge transport properties of the material and thus optimize the spectral response.

In previous work, we have shown that the specific design of the grid electrodes can affect the spectral performance of the detector. It was demonstrated that charge induction non-uniformities across the detector, due to the effect of finite detector size, can be compensated for through a simple geometrical modification of the grid electrodes.[12] In this paper, we further illustrate the use of electrode design to control the charge induction on the sensing electrodes. After a description of the conventional coplanar-grid technique, a variation of the technique is introduced which requires the measurement of the induced charge signal on only one of the grid electrodes. The optimal signal response is achieved in this case by adjusting the relative areas of the two grid electrodes. By changing the relative area of the sensing grid electrode, the charge induction characteristics of that electrode can be varied to obtain a uniform detector response for the specific carrier transport properties of the detector material. This single-electrode-readout technique requires only one amplifier and thus gives reduced electronic noise. Following a theoretical analysis of the single-electrode-readout technique, experimental measurements made with CdZnTe detectors based on this technique are presented. Induced charge signals from alpha particles demonstrate the control of the charge induction with adjustment of the grid area. The spectral performance achievable with the detectors after bias optimization is shown by ^{137}Cs spectra measured with the detectors.

2. COPLANAR-GRID TECHNIQUE AND SINGLE-ELECTRODE READOUT

The geometry of the conventional coplanar-grid detector is shown in Fig. 1. The electrodes of this detector consist of a full-area contact placed on one side of the detector and a set of two interdigitated grid electrodes patterned on the opposing detector surface. In the normal mode of operation, a large bias V_b is applied between the full contact and the grid electrodes so

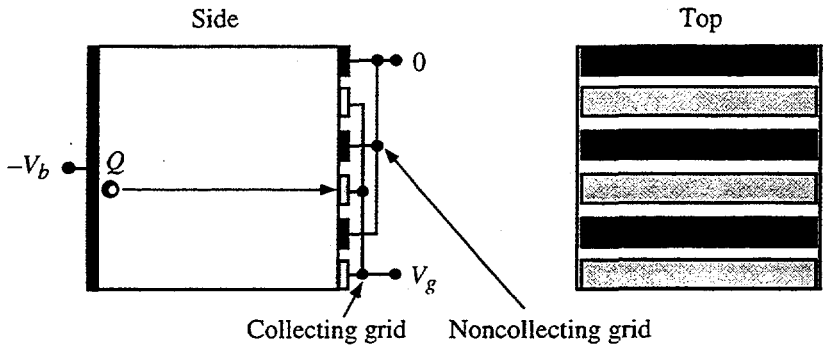

Figure 1. Schematic drawing of a coplanar-grid detector.

that the charge carriers created by radiation interactions are collected across the detector. The bias polarity is such that the electrons would drift towards the grid electrodes. A bias V_g is also applied between the two grid electrodes to ensure that these electrons would only be collected on one of the grids, referred to as the collecting grid. This bias is small relative to that applied across the detector so that the field within the bulk of the detector remains substantially uniform.

In one of the simplest grid configurations, the individual grid lines of each grid are of identical width and equal spacing. Consider a charge Q drifting in such a detector from the full-area electrode in a straight trajectory to one of the collecting grid lines, as schematically shown in Fig. 1. The charge induced on the detector electrodes as a result of the drifting charge can be determined through the weighting potential method, which has been discussed in detail elsewhere and only a brief description is given here.[13,14] The weighting potential, V_w, for a specific electrode is the electrostatic potential produced by assuming that this electrode is at unit potential, all other electrodes are at zero potential, and no space charge exists. From this potential, the charge induced on the electrode due to a charge Q at location x is $-QV_w(x)$. However, the value of interest here is the change in the induced charge signal in the measurement circuit, ΔQ_m. This is the amount of charge removed from the electrode as a result of the movement of Q within the detector, and hence is the negative of the change in the induced charge on the electrode, $\Delta Q_m = Q\Delta V_w(x)$.

The result of such a calculation for the induced charge signals from the two grids assuming no charge trapping is shown in Fig. 2(a). The two signals are the same until the charge drifts near the grids, at which point the signal from the collecting grid rapidly increases to Q and that from the noncollecting grid decreases to zero. This behavior can be understood based on the idea that the charge induced on an electrode is proportional to the number of electrostatic field flux lines connecting the drifting charge to the particular electrode. For the case when Q is far from the grids, the flux lines will be evenly distributed

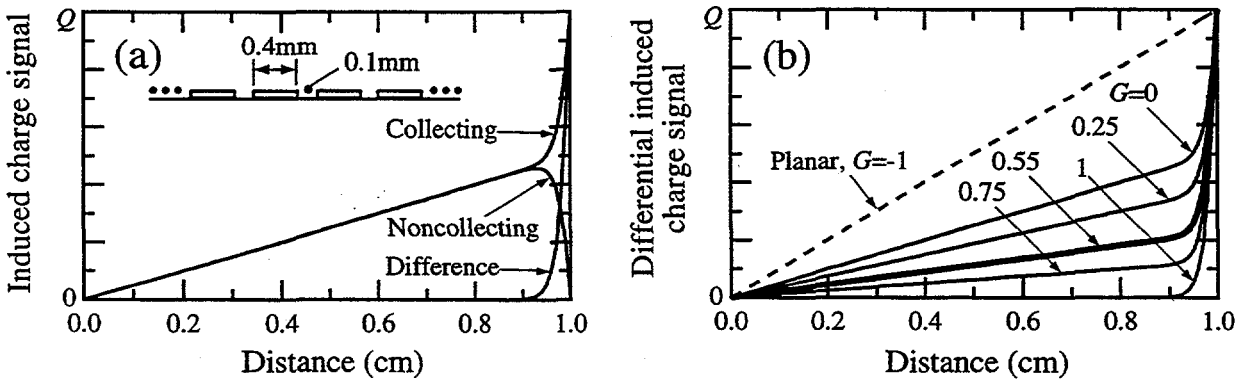

Figure 2. (a) Calculated induced charge signals on the grid electrodes of a coplanar-grid detector as a function of the distance traveled by a charge Q originating near the full-area electrode and ultimately collected on the collecting grid as illustrated in Fig. 1. The detector is assumed to be 1 cm thick and infinite in size in the lateral dimensions, and the line width of the grid electrodes are 0.4 mm with a gap spacing of 0.1 mm. Charge trapping has not been included in the calculation. The difference between the collecting and noncollecting grid signals is also plotted. This difference signal is independent of the charge motion through most of the detector volume. **(b)** Difference between the collecting and noncollecting grid signals of (a) for various values of G, which is the fraction of the noncollecting grid signal subtracted from that of the collecting grid. By adjusting G the amount of charge induction in the far-grid region can be varied. The linear induced charge signal that would result in a planar detector is shown for comparison.

between the two grids because of their interdigitated pattern and their identical size. As the charge moves towards the grids, the density of the flux lines terminating on the grids increases yet remains equally shared between the two grids. However, when the charge drifts into the region very near the grids, it becomes much closer to the particular collecting grid line on which collection will ultimately take place relative to the distance to the other grid lines. The number of flux lines terminating on this collecting grid line will then rapidly increase at the expense of all other grid lines, thus producing the rapid rise in collecting grid signal and the corresponding fall in noncollecting grid signal. We refer to this part of the detector where there is a rapid rise in the induced charge signal as the *near-grid region* and the remainder of the detector as the *far-grid region.*

This unique charge induction response can be used to reduce the loss of spectroscopic resolution caused by poor hole collection. If the noncollecting grid signal is subtracted from that of the collecting grid, as shown in the difference curve of Fig. 2(a), the resultant signal becomes insensitive to the charge drifting in the far-grid region, and the full signal is developed only as Q drifts through the small near-grid region. This implies that during detector operation, radiation interaction events that occur in the far-grid region will result in a difference signal that is derived only from the collection of electrons through the near-grid region and is not dependent on the movement of holes towards the cathode. In this measurement scheme, the detector response is nearly independent of the depth of radiation interaction even with the lack of hole collection, with the exception being events which occur in the near-grid region.

The above analysis has neglected electron trapping which, when included, re-introduces a depth dependence to the detector response. Interaction events which take place further from the grids result in a smaller number of electrons collected through the near-grid region because of trapping. For a 1 cm thick detector constructed from high quality CdZnTe material and operated under typical bias conditions,[15] roughly 20% of the initial electron charge created near the full-area electrode by an interaction event would be trapped during collection, yet nearly all the electron charge would be collected for events occurring near the grids. This variation with interaction depth would substantially degrade the energy resolution of the detector.

One method to adjust the charge induction characteristics and correct for the electron trapping is to subtract only a fraction G of the noncollecting grid signal from that of the collecting grid.[9] The differential induced charge signal as a result of the charge Q drifting from the full-area electrode to the collecting grid is shown in Fig. 2(b) for various values of G. As the plots of Fig. 2(b) indicate, by changing G, the amount of charge induction caused by carriers drifting within the far-grid region can be varied. The adjustment of G thus allows a specific amount of charge induction to be added to compensate for the amount of charge loss due to electron trapping.

A way to characterize the uniformity of the detector response with radiation interaction depth is to calculate the charge induction efficiency as a function of this depth. The charge induction efficiency is the net induced charge as a result of charge collection, normalized to the charge originally created. A flat charge induction efficiency plot is indicative of a uniform response that would give optimal spectral performance. To illustrate the improved uniformity attainable through the optimization of G, we have calculated the efficiency for various values of G using a simple detector model. In this model, both hole and electron collection with uniform carrier trapping are included. The carriers are assumed to move under the influence of a uniform electric field. It is also assumed that the radiation point interactions are centered on a particular collecting grid line and that the trajectories of the resultant carriers remain centered on this grid line during collection. The charge induction efficiency does actually vary somewhat with the lateral location of the interaction event, because of the variation in the carrier trajectories, however this simplified model is useful for studying the performance variation with G and for providing an estimate of the optimum value of G. The results of such a calculation for a 1 cm thick CdZnTe detector operated at 1000 V bias and assuming material properties typical of high quality CdZnTe are plotted in Fig. 3. The highly non-uniform response of a planar detector is plotted for comparison. For the case when the two grid signals are subtracted with unity gain, $G = 1$, the detector response suffers significantly from electron trapping. By decreasing G, the response can be made more flat and ultimately optimized to produce the nearly uniform response of the $G = 0.55$ case. The deviation from a nearly perfect flat response at this optimal condition occurs primarily for interactions taking place near the electrode surfaces. Interactions that occur near the grids give a reduced induction efficiency. This happens because the electrons traverse only a portion of the main charge induction region near the grids and therefore produce a reduced signal. The induction of the remaining part of the signal relies on the hole transport out of the near-grid region. But since the hole transport is poor and significant numbers of holes become trapped before drifting out of the near-grid region, the total induced charge signal is less than that which would result if electrons alone passed completely through the near-grid region. The downward curvature of the charge induction efficiency at the other side of the detector, near the cathode, is also the result of hole transport. With $G < 1$, the hole contribution to the induced charge signal is no longer zero in the far-grid region. For interaction events away from the electrode surfaces, this contribution is essentially independent of interaction location since the holes on average travel a short distance and then become trapped before reaching the cathode. However, near the cathode, some of the holes can reach the contact before traveling this trapping length and thus contribute a smaller amount to the net induced charge. This leads to the reduction in charge induction efficiency towards the cathode. This near-cathode effect extends further into the detector as the hole transport characteristics are improved. Also, the magnitude of the variation increases with reduced G.

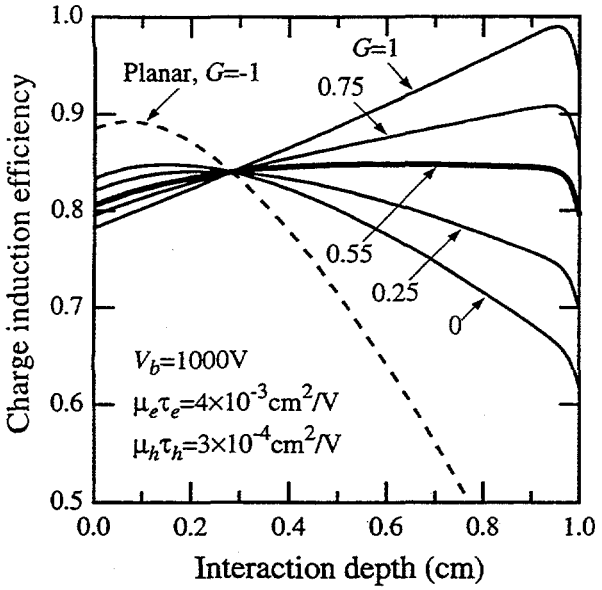

Figure 3. Calculated charge induction efficiency as a function of radiation interaction depth as measured from the full-area electrode for the coplanar-grid detector described in Fig. 2. The bias applied across the detector and the electron and hole mobility-lifetime products ($\mu_e\tau_e$ and $\mu_h\tau_h$, respectively) are listed in the figure. The charge induction efficiency is plotted for a number of values of G. For this detector and applied bias, $G = 0.55$ produces the most uniform response. The highly non-uniform response of a planar detector is shown for comparison.

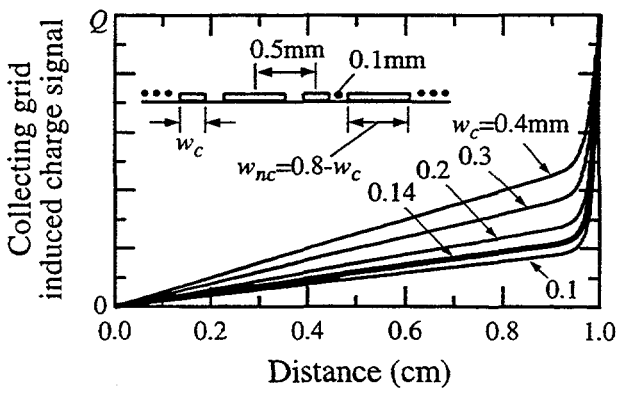

Figure. 4. Calculated induced charge signal on the collecting grid of a coplanar-grid detector as a function of the distance traveled by a charge Q originating near the full-area electrode and ultimately collected on the collecting grid. The detector is assumed to be 1 cm thick and infinite in size in the lateral dimensions. Charge trapping has not been included in the calculation. The induced charge signal is shown for a number of different collecting grid line widths, w_c. As w_c is varied, so is the noncollecting grid line width (w_{nc}) in order to maintain a constant center-to-center electrode spacing of 0.5 mm and constant gap spacing (w_g) of 0.1 mm. By adjusting the relative area of the collecting grid, the amount of charge induction can be varied.

Nevertheless, the optimization of G with respect to electron trapping improves the overall uniformity of the response and ultimately the spectral performance.

In the conventional coplanar-grid technique just described, the charge induction characteristics are adjusted to suit the particular detector material parameters and bias conditions by varying the relative gain of the two grid signals prior to subtraction. Another method to achieve a similar result is to change the geometry of the grid electrodes. For example, by decreasing the electrode area of one grid relative to the other, the induced charge on the smaller area grid as a result of charge movement within the far-grid region is reduced while that of the other grid is increased. Consider the situation where the collecting grid line width (w_c) is decreased and the noncollecting grid line width (w_{nc}) is increased such that the center-to-center spacing of the grid lines and the gap between the lines (w_g) both remain constant. With this assumption, we have calculated the induced charge signal from the collecting grid as a result of a charge Q drifting from the cathode to the collecting grid for various electrode widths. The results are shown in Fig. 4. The rate of charge induction before Q reaches the near-grid region decreases as the collecting grid line width decreases. The corresponding signals (not shown) for the noncollecting grid would show the rate of charge induction increasing. Again, the charge induction characteristics can be qualitatively understood by using the electrostatic-flux-line argument. When Q is drifting within the far-grid region and the electrode widths are the same ($w_c = w_{nc} = 0.4$ mm), the charge induction is the same for the two grids because the flux lines are equally distributed between the two grid sets. When the collecting grid line width is reduced relative to that of the noncollecting grid, fewer flux lines will terminate on the collecting grid, since it simply occupies a smaller area of the detector surface, while that of the noncollecting grid will increase. The induced charge and the rate of charge induction in the far-grid region will therefore decrease on the collecting grid. The charge induction within the near-grid region behaves similarly as before in that the induced charge signal rapidly rises to Q.

In comparing the induced charge signals of Fig. 4 to those of Fig. 2(b), it becomes clear that by changing the electrode widths we can obtain charge induction signals from one grid electrode that resemble those realized through signal subtraction. In this example, the single-grid signal obtained with $w_c = 0.14$ mm matches that of the optimal differential signal measured using the conventional coplanar-grid technique with $G = 0.55$. Optimal detector performance can therefore be achieved by measuring the induced charge signal from only the collecting grid electrode, in contrast to the conventional coplanar-grid technique which required the measurement and subsequent subtraction of both grid signals. This new *single-electrode-*

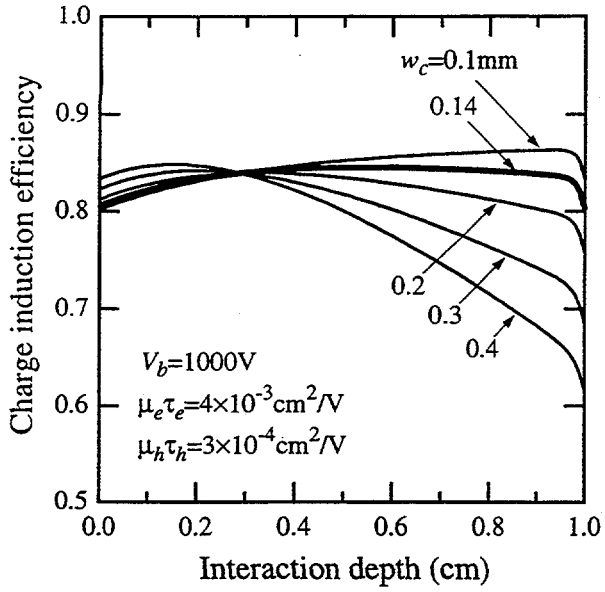

Figure 5. Calculated charge induction efficiency as a function of radiation interaction depth as measured from the full-area electrode for the single-electrode-readout coplanar-grid detector described in Fig. 4. The charge signal used in the calculation is that from only the collecting grid electrode. The charge induction efficiency is plotted for a number of collecting grid line widths. The uniformity of the detector response depends on the relative areas of the grid electrodes and, for this detector and applied bias, w_c = 0.14 mm produces the most uniform response.

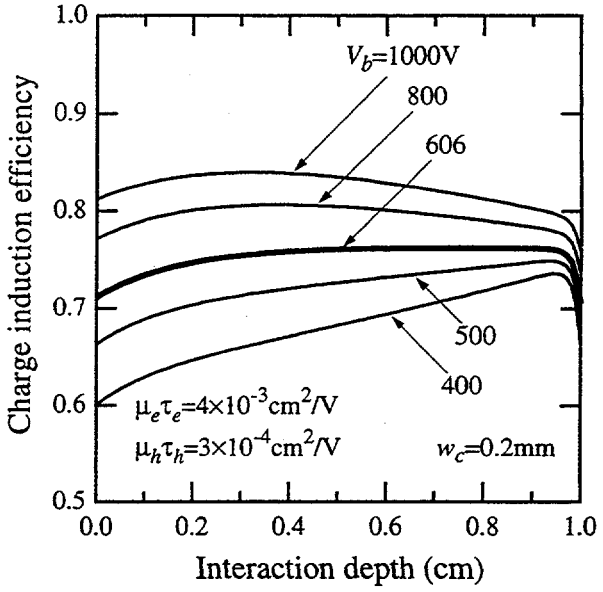

Figure 6. Calculated charge induction efficiency as a function of radiation interaction depth as measured from the full-area electrode for the single-electrode-readout coplanar-grid detector described in Fig. 4. The charge signal used in the calculation is that from only the collecting grid and the assumed collecting grid line width is 0.2 mm. The charge induction efficiency is plotted for a number of detector bias values. The uniformity of the detector response can be adjusted with the bias and the optimal value for this detector is 606 V.

readout technique has the advantages that first, the measurement electronics are simpler since a conventional single-amplifier system can be used. Second, the electronic noise will be less because the noise contribution from one of the two amplifiers required in the conventional coplanar-grid technique is eliminated.

To further substantiate that detector performance can be optimized by adjusting the electrode width ratio, in Fig. 5 is shown the charge induction efficiency of a single-electrode-readout coplanar-grid detector for the electrode configurations of Fig. 4. The efficiency has been calculated with the same simple detector model used to obtain the data of Fig. 3. By reducing the collecting grid line width to 0.14 mm and increasing that of the noncollecting grid to 0.66 mm, a reasonably flat charge induction efficiency results with a uniformity nearly identical to that of the optimized conventional coplanar-grid detector.

In practice, it is difficult to pre-determine the electrode widths that would perfectly optimize the detector for single-electrode readout. This would require a precise measurement of the detector material carrier transport characteristics combined with detailed simulations of the detector response. Fortunately, the optimum detector configuration also depends on the detector bias. By changing the bias applied across the detector, the extent of electron trapping is varied and can be made to match that needed for optimum performance given a specific grid geometry. This is illustrated in Fig. 6 in which the charge induction efficiency for the w_c = 0.2 mm case is plotted for a number of bias values. From the previous figure, Fig. 5, it is clear that w_c = 0.2 mm does not produce the optimal detector performance at a bias of 1000 V. But, from Fig. 6, we see that the performance of this case can be greatly improved by decreasing the bias to 606 V. The charge induction efficiency becomes approximately as flat as that of the optimum electrode width for operation at 1000 V (Fig. 5, w_c = 0.14 mm case). A negative consequence of a smaller optimum bias is that more electron trapping takes place and thus a smaller fraction of the total created charge is actually collected. Even though the absolute variation in the charge induction efficiency as a function of depth is approximately the same for the two optimized detectors, the one whose optimum bias is lower will have poorer detector performance in part because the fractional variation in charge induction is larger. Lower bias operation also increases the detrimental effects to spectral performance caused by spatial variations of charge transport within the detector material and ballistic deficits in the measurement electronics. A plot of optimum bias as a function of collecting grid line width for the cases of Fig. 4 is shown in Fig. 7.

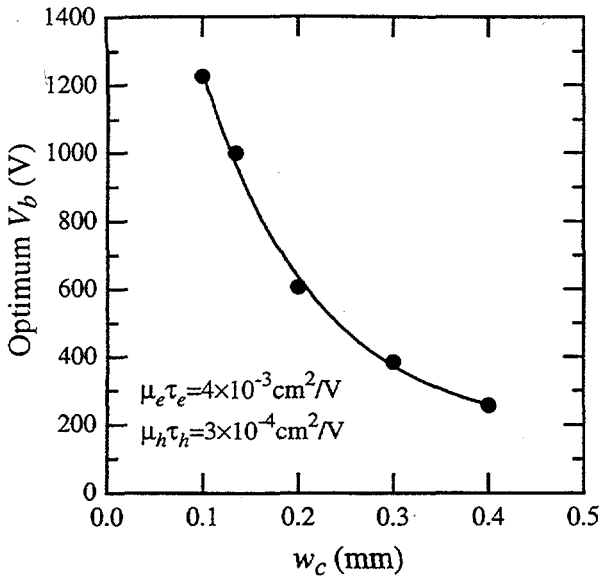

Figure 7. Optimum detector bias calculated as a function of collecting grid line width for the single-electrode-readout coplanar-grid detector described in Fig. 4. The optimum bias is that which produces the most uniform charge induction efficiency as a function of the radiation interaction depth. Reducing w_c decreases the relative area of the collecting grid and, consequently, the amount of charge induction on this grid as a result of charge drifting in the far-grid region. Therefore, the optimum bias increases since a smaller amount of electron trapping is necessary in order to match the decreased charge induction.

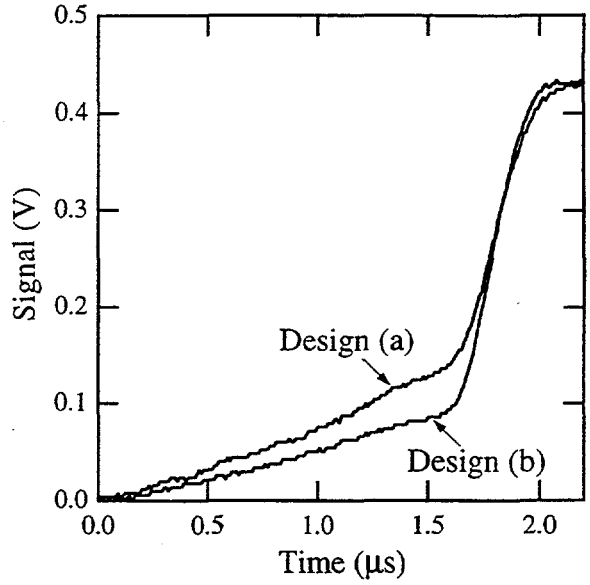

Figure 8. Measured induced charge signals on the collecting grid of a single-electrode-readout coplanar-grid detector for two different grid designs. The pulses were generated by illuminating the full-area electrode with an ^{241}Am alpha-particle source. The same CdZnTe crystal of size $9.5 \times 9.5 \times 8$ mm^3 was used for both designs and the measured mobility-lifetime products for the carriers of this crystal are $\mu_e\tau_e = 4.1\times10^{-3}$ cm^2/V and $\mu_h\tau_h = 3.5\times10^{-4}$ cm^2/V. The bias applied across the detectors was 370 V. The electrode widths and gap sizes for design (a) are $w_c = 0.25$ mm, $w_{nc} = 0.75$ mm, and $w_g = 0.25$ mm, and those for design (b) are $w_c = 0.15$ mm, $w_{nc} = 0.97$ mm, and $w_g = 0.18$ mm. The relative area of the design (a) collecting grid electrode is greater than that of the design (b) collecting grid electrode, therefore the charge induction during the majority of the charge collection process is greater for design (a).

3. EXPERIMENTAL RESULTS

Experiments were performed with single-electrode-readout coplanar-grid detectors fabricated from CdZnTe. The detector fabrication process consisted of first mechanically polishing the CdZnTe crystal with alumina powder to produce smooth surfaces. The surface damage caused by the mechanical processing was then removed by chemically etching the crystal in a 2% bromine-methanol solution immediately prior to electrode deposition. Next, gold electrodes were vacuum deposited from a heated tungsten filament, with the grid structure being defined using a shadow mask. Finally, electrical connection was made to the grid electrodes by bonding a gold wire to each individual grid line with silver epoxy. The epoxy was cured at approximately 55°C for 16 h.

The charge induction characteristics of the detectors were characterized by exposing the full-area cathode electrode of each detector under vacuum to an ^{241}Am alpha-particle source, so that the induced signal resulted solely from electron collection across the entire thickness of the detector. The collecting grid signals from detectors with two different grid designs are compared in Fig. 8. The same CdZnTe crystal of size $9.5 \times 9.5 \times 8$ mm^3 has been used for both designs to avoid differences in the measured characteristics caused by material variations. As expected from the previous theoretical discussion, when the drifting electrons are passing through the far-grid region, the charge induction is dependent on the relative grid areas. Grid design (a) with the wider collecting grid lines and thinner noncollecting lines results in a greater amount of far-grid signal as compared to that of design (b).

The gamma-ray spectral responses to a ^{137}Cs source for the two detectors are shown in Fig. 9. For comparison the response of the detector when operated as a simple planar detector is also plotted. All three spectra were measured using the same amplifier. The spectral performance of the planar detector is very poor with only a shoulder present in the spectrum at the 662 keV gamma-ray energy. In contrast, the single-electrode-readout coplanar-grid detectors both exhibit a sharp gamma-

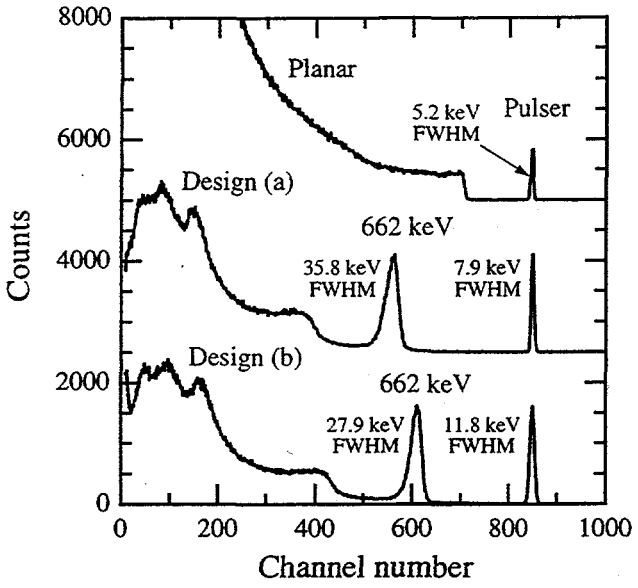

Figure 9. Measured spectra of ^{137}Cs obtained with the single-electrode-readout coplanar-grid detectors described in Fig. 8. The poor spectral response of a planar detector is shown for comparison. All three detector configurations were each implemented on the same CdZnTe crystal and all of the spectra were acquired using the same amplifier. The operating biases for the single-electrode-readout detectors were adjusted to optimize their spectral performance. The detector biases for the design (a) detector were $V_b = 370$ V and $V_g = 30$ V, and those for design (b) were $V_b = 500$ V and $V_g = 40$ V. The bias applied across the planar detector was 1000 V. Since the design (b) detector is optimized at a higher detector bias than that of the design (a) detector, the design (b) detector resolves the 662 keV gamma-ray peak better than the other design.

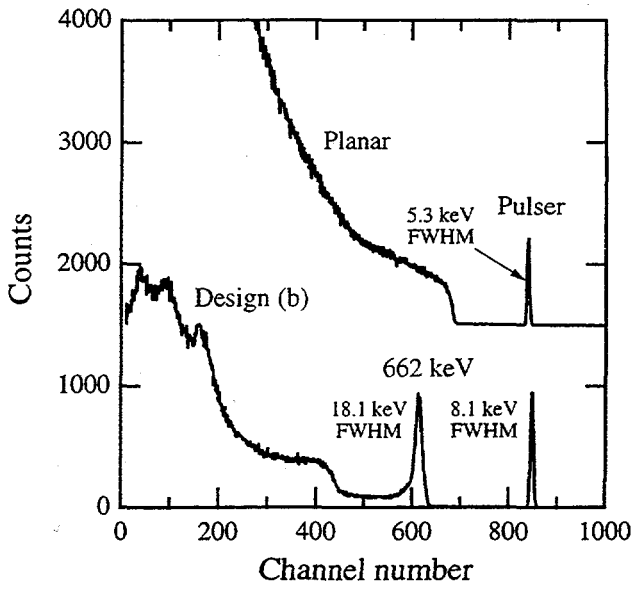

Figure 10. Measured spectrum of ^{137}Cs obtained with a single-electrode-readout coplanar-grid detector of the design (b) described in Fig. 8. The planar detector response for the CdZnTe crystal used to make this detector is shown for comparison. The CdZnTe crystal is $10 \times 10 \times 7$ mm^3 in size and has a measured electron mobility-lifetime product that is a factor of 0.6 times that measured for the crystal used to obtain the results shown in Fig. 9. The optimized detector biases used with the design (b) detector were $V_b = 880$ V and $V_g = 40$ V. The bias applied across the planar detector was 1000 V.

ray peak and a well-defined Compton edge. The operating biases of the single-electrode-readout detectors were adjusted to produce the narrowest gamma-ray peak width possible. The detector of design (b) with the higher optimum bias yields a sharper gamma-ray peak as expected. However, the optimal bias for design (b) is still quite low and we would expect to achieve even better performance with this CdZnTe crystal using a design with an even smaller relative area for the collecting grid and hence less compensation for electron trapping.

To demonstrate the importance of the material carrier transport properties on determining the best detector design, we have used the design (b) grid pattern on another CdZnTe crystal which has a measured electron mobility-lifetime product that is approximately 0.6 times that of the detector crystal already discussed. The ^{137}Cs spectrum measured with this detector is shown in Fig. 10 with the planar detector response shown for comparison. Since the electron transport of this material is poorer than that of the Fig. 9 material, a higher detector bias is required in order to match the amount of electron trapping to the compensation provided by the electrode design. The larger optimum bias probably contributes to the better resolution of this detector.

The single-electrode-readout technique using conventional detector electronics can clearly be used to produce detectors with good spectroscopic resolution. However, there are some additional considerations with this technique. First, the detector fabrication may become more difficult when the electrode designs are optimized for higher bias operation or when material with good electron transport is used, since this would require a small collecting to noncollecting grid line width ratio.[16] This could be accomplished by increasing the noncollecting grid line width, but this then increases the center-to-center grid line spacing. This spacing dictates the size of the near-grid region which has a highly non-uniform response to gamma-ray interactions. As the spacing is increased so is the near-grid region leading to a loss of spectral performance. A better alternative is to decrease the line width of the collecting grid. The small line width required of the collecting grid though will probably make it necessary to use more complex electrode fabrication and lead attachment processes than those used in this study.

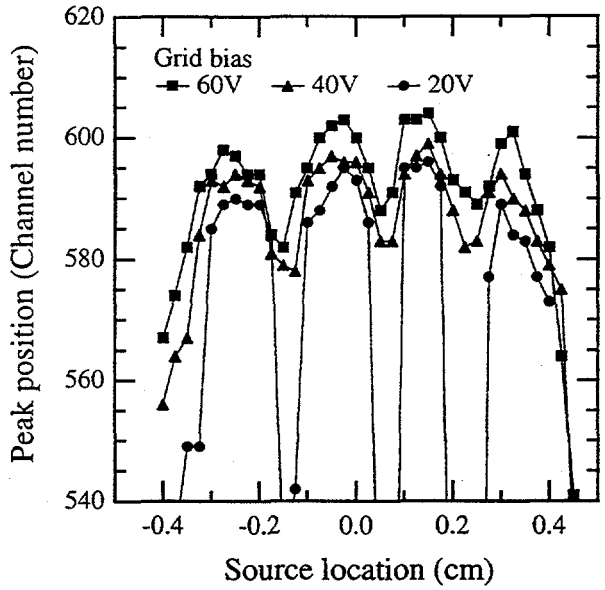

Figure 11. Alpha-particle peak position plotted as a function of source location for the single-electrode-readout coplanar-grid detector of the design (b) whose gamma-ray spectral response is shown in Fig. 9. The data was obtained by scanning a collimated ^{241}Am alpha-particle source along the full-area electrode of the detector and measuring the energy spectrum at many locations along the scan. The scan direction was perpendicular to the lines of the grid electrodes. The bias applied across the detector was $V_b = 500$ V and the measurement was made for three different grid biases as indicated in the figure. The periodic fluctuations in the peak position are most likely due to the variations in the electron trajectory path lengths caused by the coplanar-grid structure.

Another consideration with the technique is illustrated in Fig. 11. The data of this figure was obtained by scanning a collimated ^{241}Am alpha-particle source along the full-area cathode of a design (b) detector, in a direction that is perpendicular to the grid lines. Energy spectra were collected at various source locations along the detector and the position of the alpha peak in each spectrum was recorded. Figure 11 is a plot of the alpha-particle peak position as a function of the source location for a number of grid biases. A variation in the peak position indicates a change in the charge induction. Since the observed variation is periodic with a period that is roughly the center-to-center spacing of the collecting grid lines, the change primarily results from the grid structure rather than non-uniformities of the detector material. A reasonable explanation for this is based on the electron collection time being dependent on the particular trajectory that the charge follows. If, for example, the alpha-particle interaction event takes place directly beneath a collecting grid line, the trajectory of the resultant electrons will be roughly a straight line to this particular grid line with a path length approximately equal to the detector thickness. In contrast, an event occurring directly beneath a noncollecting grid line results in a longer path length since the electrons must change course near the grids to reach the collecting grid. Such electrons may also pass through a low electric field region near the grids. The charge from this type of an event therefore has a longer collection time and will suffer from more electron trapping, leading to a smaller detector signal. The magnitude of the variations for the grid biases of 40 V and 60 V is consistent with this explanation. The large dips observed with the small grid bias, 20 V, probably are caused by charge sharing between the collecting and noncollecting grids. The above argument then implies that gamma-ray interactions which occur at the same depth within the detector will also suffer from a spread in electron trajectory lengths causing a loss of energy resolution. This again indicates that a small center-to-center grid line spacing is desirable.

4. CONCLUSIONS

We have shown that by properly designing the charge collection grid of a coplanar-grid detector, good spectroscopic performance can be achieved by measuring the induced charge signal from only this grid. A reduction in electronic noise and the ability to use conventional single-amplifier detection electronics results. Key to the success of this single-electrode-readout technique was shown to rely on designing the grid electrodes such that the optimum operating bias is sufficiently large. To achieve this, it is more desirable to decrease the collecting grid size rather than increasing the size of the noncollecting grid in order to maintain a small center-to-center grid line spacing.

ACKNOWLEDGMENTS

This work was supported by the Director, Office of Energy Research, Biological and Environmental Research, of the U.S. Department of Energy under Contract No. DE-AC03-76SF00098.

REFERENCES

1. E. Sakai, "Present status of room temperature semiconductor detectors", *Nucl. Instr. Meth.* **196**, pp. 121-130, 1982.

2. J. F. Butler, C. L. Lingren, and F. P. Doty, "$Cd_{1-x}Zn_xTe$ gamma ray detectors", *IEEE Trans. Nucl. Sci.* **39**, pp. 605-609, 1992.

3. *Semiconductors for Room Temperature Nuclear Detector Applications*, *Semiconductors and Semimetals* **43**, edited by T. E. Schlesinger and R. B. James, Academic Press, New York, 1995.

4. *Semiconductors for Room-Temperature Radiation Detector Applications*, *Materials Research Society Symposium Proceedings* **302**, edited by R. B. James, T. E. Schlesinger, P. Siffert, and L. Franks, Materials Research Society, Pittsburgh, 1993.

5. H. L. Malm, C. Canali, J. W. Mayer, M-A. Nicolet, K. R. Zanio, and W. Akutagawa, "Gamma-ray spectroscopy with single-carrier collection in high-resistivity semiconductors", *Appl. Phys. Lett.* **26**, pp. 344-346, 1975.

6. P. N. Luke, "Single-polarity charge sensing in ionization detectors using coplanar electrodes", *Appl. Phys. Lett.* **65**, pp. 2884-2886, 1994.

7. P. N. Luke, "Unipolar charge sensing with coplanar electrodes – application to semiconductor detectors", *IEEE Trans. Nucl. Sci.* **42**, pp. 207-213, 1995.

8. H. H. Barrett, J. D. Eskin, and H. B. Barber, "Charge transport in arrays of semiconductor gamma-ray detectors", *Phys. Rev. Lett.* **75**, pp. 156-159, 1995.

9. P. N. Luke and E. E. Eissler, "Performance of CdZnTe coplanar-grid gamma-ray detectors", *IEEE Trans. Nucl. Sci.* **43**, pp. 1481-1486, 1996.

10. P. N. Luke, "Electrode configuration and energy resolution in gamma-ray detectors", *Nucl. Instr. Meth. Phys. Res.* **A 380**, pp. 232-237, 1996.

11. Z. He, G. F. Knoll, D. K. Wehe, and J. Miyamoto, "Position sensitive single carrier CdZnTe detectors", *1996 IEEE Nuclear Science Symposium Conference Record*, edited by A. Del Guerra, pp. 331-335, 1997.

12. P. N. Luke, M. Amman, T. H. Prettyman, P. A. Russo, and D. A. Close, "Electrode design for coplanar-grid detectors", *IEEE Trans. Nucl. Sci.*, accepted for publication.

13. W. Shockley, "Currents to conductors induced by a moving point charge", *J. Appl. Phys.* **9**, pp. 635-636, 1938.

14. S. Ramo, "Currents induced by electron motion", *Proc. I. R. E.* **27**, pp. 584-585, 1939.

15. An electron mobility-lifetime product of 4×10^{-3} cm^2/V and bias of 1000 V were assumed.

16. The width of the gap is also important in determining the amount of compensation for electron trapping. If it is assumed that the weighting potential varies linearly between the grid lines at the detector surface, then the rate of charge induction on the collecting grid is proportional to $(w_c + w_g)/(w_c + w_{nc} + 2w_g)$, for charges drifting within the far-grid region. The linear potential assumption is actually not correct and this result is only an approximation, however it can still be concluded that to have the charge induction on the collecting grid be small, it is necessary to have a small gap between the grid electrodes.